CHEMISTRY
AN ASIAN JOURNAL

DOI: 10.1002/asia.200900274

Concentration Dependent Transformation of Oligopeptide based Nanovesicles to Nanotubes and an Application of Nanovesicles

Jishu Naskar and Arindam Banerjee*[a]

Abstract: The concentration dependent transformation of an oligopeptide nanostructure from nanovesicles to nanotubes at neutral pH is presented. The oligopeptide Acp-Tyr-Glu (Acp: 6-aminohexanoic acid) forms nanovesicles at a concentration of 6.9 mg mL^{-1}. At a concentration of 2.3 mg mL^{-1} these vesicular structures completely disappear and nanotubular structures are observed. We have also successfully optimized an intermediate concentration (3.4 mg mL^{-1}) where an ordered array of fused vesicular structures are formed, which actually leads to the transition from nanovesicles to nanotubes. These vesicular structures are very much sensitive toward metal ions and pH. Biocompatible calcium ions and high pH (10.7) can trigger the rupturing of these nanovesicles. One important property of these nanovesicular structures is the encapsulation of a potent anticancer drug doxorubicin, which can also be released in the presence of calcium ions promising a future use of these nanovesicles as vehicles for carrying biologically important molecules.

Keywords: fluorescence · nanotubes · oligopeptide · self-assembly · vesicles

Introduction

Molecular self-assembly has emerged as a powerful tool for making various nanostructures and this leads to the development of advanced materials.[1] Manipulation of nanoscale structures can be performed with precision by the proper selection of molecular building blocks and the control of their self-assembly. Molecules, such as lipids,[2a] amino acid derivatives,[2b] peptides,[2c,d,e,f] and proteins play an increasingly important role for this purpose. Peptide based scaffolds are very interesting candidates for constructing nanostructures owing to their well-defined structure,[2c,d,e,f,h] biocompatibility,[3] and molecular recognition property.[2b,4] There are numerous examples of short acyclic peptide based nanotube formation. The first example of simple dipeptide based nanotube formation in crystal was reported by Görbitz and these nanotubes have chiral hydrophilic channels with van der Waals diameter up to 10 Å.[2a] Gazit et al. reported that a very short peptide, diphenylalanine (Phe–Phe), the aromatic core of β-amyloid polypeptide, can be self-assembled to form a novel class of peptide nanotubes. These nanotubes have a long length and unique mechanical properties with a Young's modulus of about 19 GPa.[5] These peptide nanotubes not only can serve as a degradable mold for the fabrication of silver nanowires[3c] but also enable the formation of platinum nanoparticle composites.[3a] Recent study has demonstrated that a peptide nanotube can be used as a part of an electrochemical biosensor platform.[6] By varying the self-assembling building block, nanostructural transformation can be performed from spherical to tubular or cylindrical.[7] There are a few reports of chirality induced unprecedented transition from vesicles to helical tubules.[8] Gazit et al. have reported the dipeptide based nanotube to hollow nanocage structural transition observed by simply attaching a thiol group at the terminal position of the dipeptide.[9] Other examples of peptide based nanostructural transitions include pH-sensitive[10] and concentration dependent[11] transformation of nanotubes to nanovesicles using the controlled self-association of a singular peptide building block. Shelnutt and co-workers have reported the synthesis of dipeptide nanotubes (DPNTs) using nanopure water instead of fluoropropanol and they observed that these nanotubes turned into vesicles upon dilution using water.[3a] Zhang and co-workers reported several surfactant-like oligopeptides (each with ~2 nm in length) undergo self-assembly to form

[a] J. Naskar, Dr. A. Banerjee
Department of Biological Chemistry
Indian Association for the Cultivation of Science
Jadavpur, Kolkata-700032, West Bengal (India)
Fax: (+91) 33-24732805
E-mail: bcab@iacs.res.in
arindambolpur@yahoo.co.in

Supporting information for this article is available on the WWW under http://dx.doi.org/10.1002/asia.200900274.

nanotubes and nanovesicles having an average diameter of 30–50 nm.[3b] Li et al. reported that a positively charged dipeptide nanotube (H-Phe-Phe-NH_2·HCl) undergoes a spontaneous conversion into vesicles upon dilution at physiological condition. These positively charged nanotubes with fluorescently labeled ssDNA could enter cells readily after their conversion into vesicles with attached ssDNA.[11] This transition is reversible in nature.[12] A recent study also demonstrated the structural regulation of tubes into vesicles by molecular coassembly manipulated by a charge-transfer interaction.[13] In our laboratory, we are involved in studying the self-assembly of short synthetic peptides into various nanoscopic species including nanotubes,[14a] nanorods,[14b] nanovesicles,[10] and the transition of one nanostructure into the other.[10] However, the self-assembly of short synthetic peptides into well defined nanostructures and the breaking of these nanostructures by interaction with biocompatible metal ions like Ca^{2+}, Mg^{2+}, K^+, and so forth, is very interesting. To the best of our knowledge this type of study is very rare in the literature.[15] This report describes the self-assembly of short water-soluble tripeptides containing 6-aminohexanoic acid (Acp) as the N-terminal residue, Acp-Tyr-Glu (Figure 1), into nanovesicles and nanotubes at different concentrations at neutral pH. The formation of these

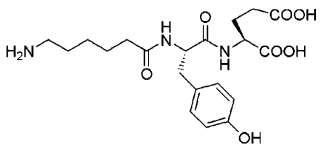

Figure 1. Chemical structure of the compound.

nanovesicles is very much sensitive toward metal ions and pH. The presence of biocompatible Ca^{2+} ions and high pH, trigger the rupturing of these nanovesicles. These nanovesicles can encapsulate a potent anticancer drug (doxorubicin) and the drug can be released in the presence of Ca^{2+} ions by rupturing these vesicles indicating a probable use as a nanovehicle for carrying drugs and other biologically important molecules.

Results and Discussion

To access the formation of supramolecular structures through molecular self-assembly, the dynamic light scattering (DLS) experiment was performed. It is a rapid screening method used to define nanostructures. Without the presence of discrete peak intensity, no nanostructure can be observed. From the DLS study, it was found that nanostructures of various sizes (within the range 80–120 nm) were formed (Figure 2a) at a peptide concentration of 6.9 mg mL^{-1}. However, at lower concentration (2.3 mg mL^{-1}) nanostructures of very narrow sizes (100–110 nm) were observed (Figure 2b). These observations encouraged us to further study these

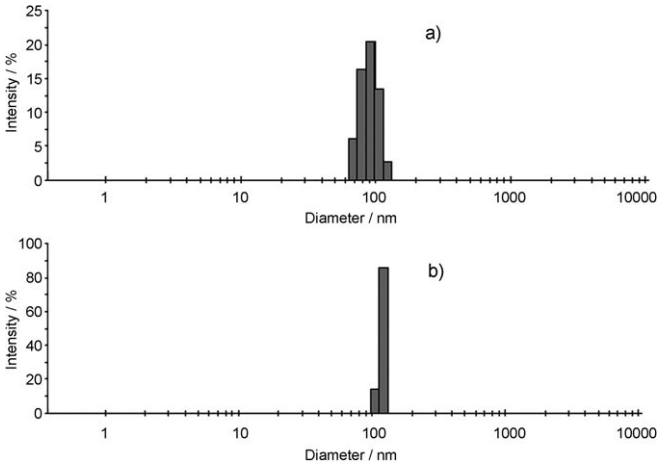

Figure 2. DLS study at peptide concentration (a) 6.9 mg mL^{-1}, (b) at 2.3 mg mL^{-1}.

structures by various electron microscopic techniques, such as SEM and TEM.

To investigate the morphological features of these self-assembled water-soluble tripeptide, a field emission scanning electron microscopic (FE-SEM) study was performed. Peptide (6.9 mg) was dissolved in 1 mL water (pH 6.96) and the solution was allowed to age for 6 h. The FE-SEM study elucidated the formation of nanospheres of various sizes (Figure 3).

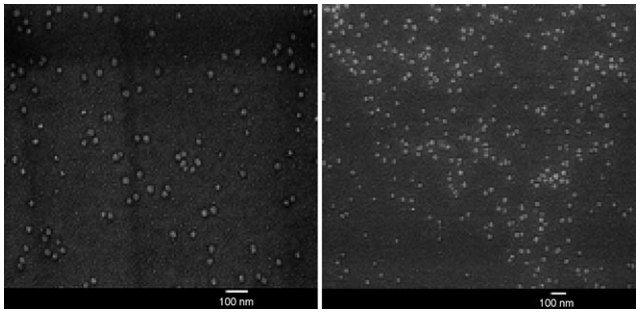

Figure 3. FE-SEM microscopic images of nanospheres at concentration 6.9 mg mL^{-1}.

To access the morphological insight of these self-assembled nanospheres, transmission electron microscopic (TEM) studies were performed. From the TEM study it was revealed that the spheres were hollow, and they form nanovesicles with diameters ranging from 30 to 80 nm (Figure 4). Figure 5 illustrates the vesicle size distribution plot showing the population of different sized vesicles formed by this water-soluble tripeptide. This distribution plot shows that exclusively vesicles having diameters between 40–60 nm have been formed.

To access an independent indication about the topography of nanostructures, atomic force microscopic (AFM) studies have been performed. The sample was deposited on a mica

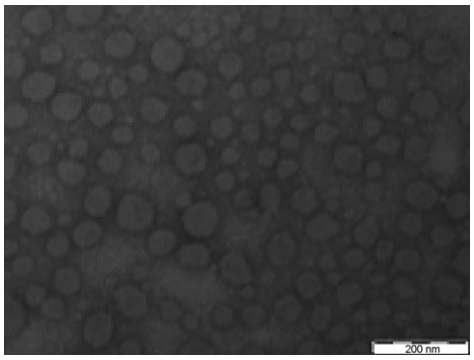

Figure 4. TEM images showing the formation of nanovesicles at concentration 6.9 mg mL^{-1}.

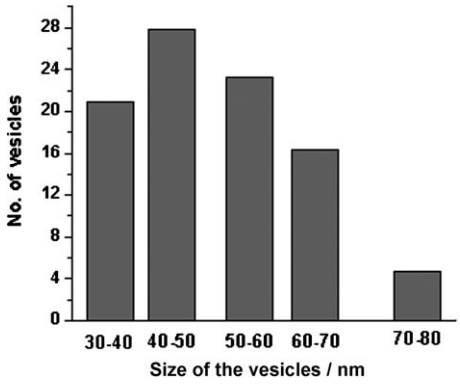

Figure 5. Vesicle size distribution plot showing the population of different size vesicles at concentration 6.9 mg mL^{-1}

surface and investigated by an atomic force microscope. The calculated height of the vesicle was about 15.34 nm (Figure 6c). All these studies confirmed that the reported tripeptide self-assembled into vesicles at a concentration of 6.9 mg mL^{-1}.

The solution of nanovesicles was diluted in such a way that the final concentration was 2.3 mg mL^{-1}. After aging this solution for 6 h, transmission electron microscopic studies were performed and it was observed that tubular structures were formed with an average diameter of 70 nm and the length of these tubes was ~2.5 μm (Figure 7a–d).

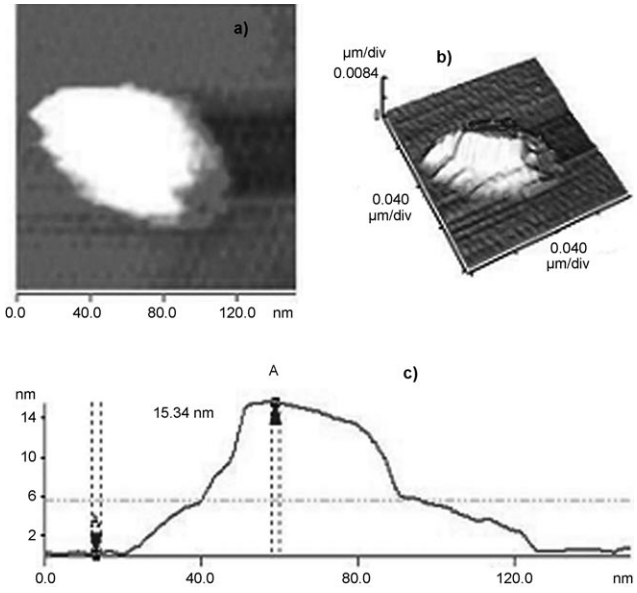

Figure 6. Atomic force microscopic image of vesicle (a), topographic view along z-axis (b), height profile plot (c).

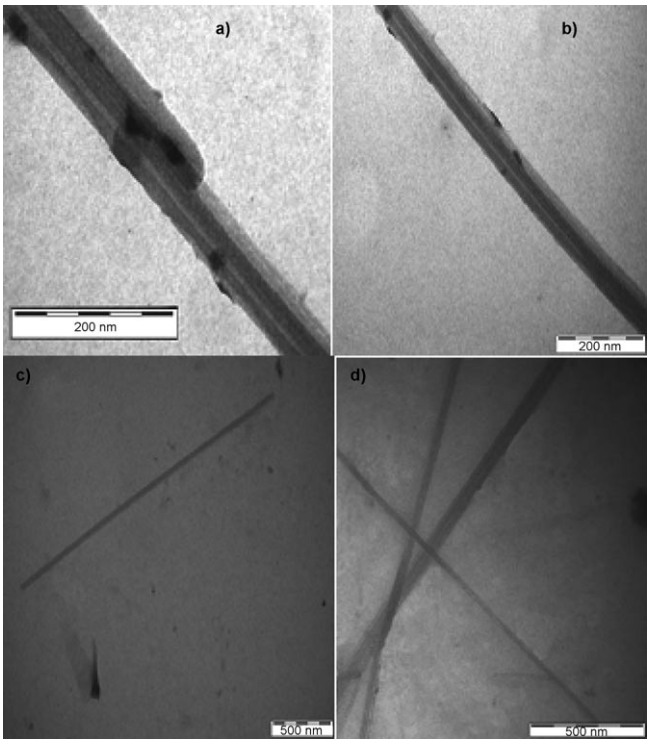

Figure 7. TEM images of nanotubular structure formed at peptide concentration 2.3 mg mL^{-1}. (a) and (b) showing a single nanotube with a hollow channel, (c) showing the length of a tube, (d) showing the coexistence of more than one nanotube.

For further clarification of this transition the stock peptide solution (6.9 mg mL^{-1}) was diluted to make a final concentration of 3.45 mg mL^{-1}. This diluted solution was aged for 3 h and then transmission electron microscopic studies were performed. Interestingly, the formation of an ordered array (Figure 8) of fused nanovesicles were observed. Here it can be thought that the vesicle to tube transition passes through an intermediate structure of a fused orderly aligned array of nanostructures, as depicted in Figure 8. TEM experiments were also performed using samples with a concentration of 12 mg mL^{-1} (above 6.9 mg mL^{-1}) as well as at a concentration below 2.3 mg mL^{-1} (1.6 mg mL^{-1}) to investigate whether any new nanofeature is observed. However, vesicular morphology is still retained at higher concentrations (12 mg mL^{-1}) and tubular morphology is also retained at lower concentration (1.6 mg mL^{-1}) (Figure S6 in the Supporting Information). It is interesting to note that the change in concentration plays a vital role to illustrate the

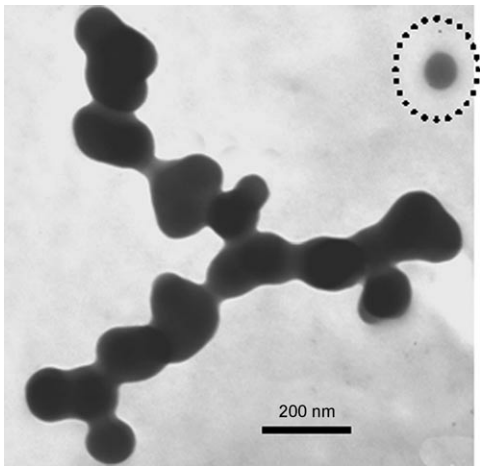

Figure 8. TEM image showing the transition of nanovesicles to nanotube at intermediate concentration (3.4 mg mL^{-1}). Circle showing an isolated vesicle.

type of nanostructure formation from the self-assembling tripeptide (Figure 9). This is a unique example of a nanovesicle to nanotube transition that is triggered by dilution.

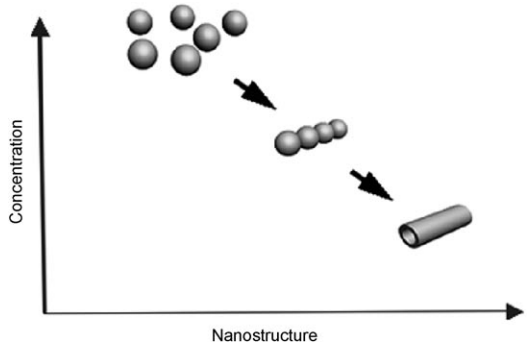

Figure 9. Schematic illustration of the concentration dependent nanostructural transformation from nanovesicles to nanotubes with the appearance of an intermediate nanostructure of orderly array of fused nanovesicles: (a) nanovesicles, (b) intermediate, orderly array of fused nanovesicles, (c) a nanotube.

An FTIR study (Figure S5 in the Supporting Information) has been performed in order to access the secondary structure of this water-soluble tripeptide at different concentrations. From the FTIR spectra, it was found that an intense peak (owing to amide I stretching) appeared at 1673 cm^{-1} and an N–H stretching frequency appeared at 3400 cm^{-1} indicating a hydrogen bonded turn (type II β turn)[16] conformation of the reported peptide at different concentrations.

Circular dichroic (CD) spectra (Figure 10) of this water-soluble tripeptide at different concentrations showed two positive bands. A band arising from an n–π* transition appeared at 225 nm (for various concentrations) and the other peaks (for π–π*) appeared at 205 and 207 nm, clearly indicating the presence of a turn-like secondary structure for

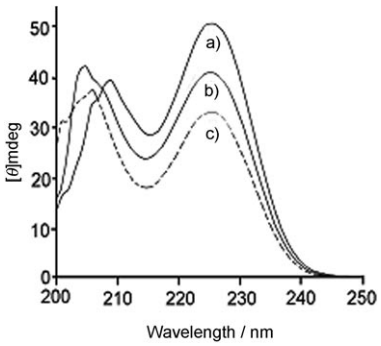

Figure 10. CD spectra of the peptide at different concentration, (a) 6.9 mg mL^{-1}, (b) 3.4 mg mL^{-1}, (c) 2.3 mg mL^{-1}.

this reported tripeptide at different concentrations[17] and this supports the data obtained from the FTIR study. Only the intensity of the peaks changed with concentration whilst the basic features of the peak remained unaltered.

It is well known that various interactions, such as hydrogen bonding, π–π interaction, and hydrophobic interactions play a significant role in the self-assembly of peptides in water and this ultimately leads to the formation of various peptide based nanostructures including nanotubes, nanorods, nanovesicles, and others.[2d,e,f,3c,10,14a,b] It is evident from CD and FTIR experiments that the reported oligopeptide Acp-Tyr-Glu has a turn structure in solution, which does not change upon dilution. Figure 11 provides a schematic repre-

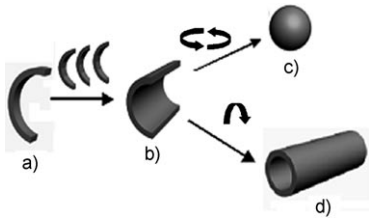

Figure 11. Schematic presentation showing a tentative model for the formation of a nanotube and a nanovesicle: (a) turn shaped molecular conformation, (b) molecular assembly having a curvature, (c) two dimensional layer closure of this curved structure generates a nanovesicle, (d) rolling of this curved structure in one direction leads to the formation a nanotube.

sentation illustrating the formation of nanovesicles and nanotubes from a curved shaped assembly. This turn structure can be self-assembled in one direction to form a curved, assembled structure (Figure 11 b). Two-dimensional layer closure of this type of curved shaped supramolecular structure leads to the formation of a vesicular structure (Figure 11 c). Furthermore, rolling up of this curved structure results in the formation of a tubular structure (Figure 11 d).[3b,9,18]

Formation of soft vesicular structures and their disruption is very important in drug delivery. For that purpose, we became interested in optimizing the condition for the rupturing of these soft vesicular structures. From the TEM

study, it was observed that the presence of biocompatible Ca^{2+} ions (at a peptide/metal ion concentration ratio 2:1) could trigger the rupturing of these nanovesicles (Figure 12a) and energy dispersive X-ray (EDX) analysis proved the presence of calcium within the ruptured vesicles (Figure S4 in the Supporting Information). We have also tested the pH sensitivity of these nanovesicles. This vesicular morphology was completely lost at pH 10.7 (Figure 12b).

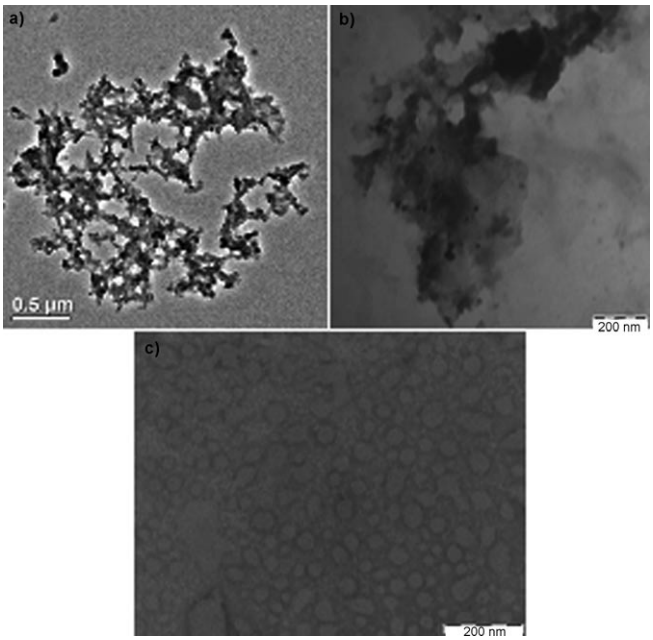

Figure 12. TEM images of ruptured nanovesicles (a) in the presence of calcium ions (b) at high pH 10.7 (c) stability of vesicles at pH 5.2.

Biomolecule based nanostructures are very promising candidates as excellent vehicles for carrying various bioactive molecules into living systems owing to their biocompatibility and tailorability for targeted delivery.[3c,9,19] There are various reports of peptide based self-assembled nanostructures. However, the encapsulation of bioactive molecules into peptide vesicles is yet to be explored. Here, a simple enclosed environment of peptide nanovesicles has been utilized for encapsulation of a potent anticancer drug, doxorubicin. In this study the peptide solution was incubated with doxorubicin for seven days to permit fluorescence detection of drug-loaded nanovesicles. Fluorescence microscopic studies clearly affirmed the drug entrapment from the appearance of fluorescent circular structures (Figure 13a) viewed under a fluorescence microscope. It is interesting to note that the entrapped drug can be released easily by adding Ca^{2+} ions into the drug loaded vesicle solution (Figure 13b). The presence of Ca^{2+} ions brings about the complete rapture of these drug-filled vesicles and allows release of the drug into the surroundings. Thus, these nanovesicles may serve as delivery vehicles for drugs and other biologically important molecules.

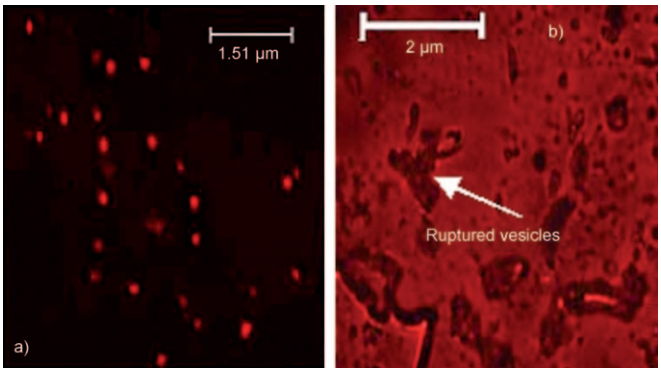

Figure 13. Confocal fluorescence microscopic image of doxorubicin loaded vesicles (a), doxorubicin released from vesicles in the presence of calcium ions (b).

Conclusions

In summary, we have described the self-assembly of a water-soluble tripeptide that leads to the formation of two nanoscopic spieces, nanovesicles and nanotubes, at neutral pH. At a peptide concentration of 6.9 mg mL^{-1}, exclusive formation of nanovesicles was observed and at 2.3 mg mL^{-1}, the peptide is self-assembled into nanotubes. This indicates that this vesicle to tube transition is concentration dependent. These peptide nanovesicles were able to entrap small drug molecules, doxorubicin. Formation of nanovesicles was very sensitive toward metal ions and pH. These vesicular structures can be ruptured in the presence of biocompatable Ca^{2+} ions and also by an increase of the pH of the solution. Calcium ion triggered rupturing of drug loaded nanovesicles holds future promise to use these nanovesicles as nanovehicles of carrying drugs to the target site.

Experimental Section

The reported peptide was synthesized by conventional solution phase methods by using recimization free fragment condensation strategy. The Boc group was used for N-terminal protection and the C-terminus was protected with a methyl ester. Deprotections of the ester group were performed using the saponification method, and removal of the Boc group with trifluoro acetic acid (TFA). Couplings were mediated by dicyclohexylcarbodiimide and 1-hydroxybenzotriazole (DCC/HOBT). The final compound was fully characterized by NMR, mass, and IR spectroscopy.

Synthesis

Boc-Acp-OH: A solution of 6-aminocaproic acid (2.62 g, 20 mM) in a mixture of dioxane (40 mL), water (20 mL), and 1 M NaOH (20 mL) was stirred and cooled in an ice water bath. Di-*tert*-butyl pyrocarbonate (4.8 g, 22 mM) was added, and stirring was continued at room temperature for 6 h. The solution was then concentrated in vacuum to about 20–25 mL, cooled in an ice-water bath, covered with a layer of ethyl acetate (about 20 mL), and acidified with a dilute solution of $KHSO_4$ to pH 2–3 (congo red). The aqueous phase was extracted with ethyl acetate, and this operation was done repeatedly. The ethyl acetate extracts were pooled, washed with water, dried over anhydrous Na_2SO_4, and evaporated in vacuum. The pure material was obtained as a waxy solid. Yield: 3.93 g (17 mM, 85%); elemental analysis: calcd (%) for $C_{11}H_{21}NO_4$ (231): C 57.79, H 9.76, N 6.06; found: C 56.77, H 9.78, N 5.99.

Boc-Acp-Tyr-OMe (1): A total of 3.69 g (16 mM) of Boc-Acp-OH was dissolved in a mixture of 25 mL of dichloromethane (DCM) in an ice water bath. H-Tyr-OMe was isolated from 7.36 g (32 mM) of the corresponding methyl ester hydrochloride by neutralization, subsequent extraction with ethyl acetate, and concentration (15 mL). This was added to the reaction mixture, followed immediately by 3.3 g (16 mM) of DCC. The reaction mixture was allowed to come to RT and was stirred for 48 h. DCM was evaporated, the residue was taken in ethyl acetate (60 mL), and dicyclohexylurea (DCU) was filtered off. The organic layer was washed with 2 M HCl (3×50 mL), brine (2×50 mL), and 1 N sodium carbonate (3×50 mL) and brine (2×50 mL), dried over anhydrous sodium sulfate, and evaporated under vacuum to yield as a white solid. Yield: 4.89 g (12 mM, 75%); ^{1}H NMR (300 MHz, [D]CHCl$_3$): δ=6.95 (d, J=9, 2H; ArH), 6.81 (d, J=9, 2H; ArH), 5.82 (d, J=6, 1H; Tyr CONH), 4.90–4.83 (m, 1H; Tyr C$^{\alpha}$H), 4.64 (b, 1H; Acp CONH), 3.77 (s, 3H; COOCH$_3$), 3.24–3.18 (m, 2H; Acp C$^{\varepsilon}$H$_2$), 3.02–2.98 (m, 2H; Tyr C$^{\beta}$H$_2$), 2.87–2.79 (m, 2H; Acp C$^{\alpha}$H$_2$), 2.16–2.05 (m, 2H; Acp C$^{\beta}$H$_2$), 1.46 (s, 9H; (CH$_3$)$_3$C), 1.40–1.28 (m, 2H; Acp C$^{\delta}$H$_2$), 1.06–1.04 ppm (m, 2H; Acp C$^{\gamma}$H$_2$); ESI-MS: 430.92 [M+Na]$^+$, 431.92 [M+H+Na]$^+$; elemental analysis: calcd (%) for $C_{21}H_{32}N_2O_6$ (408): C 61.75, H 7.90, N 6.86; found: C 50.55, H 7.96, N 6.42.

Boc-Acp-Tyr-OH (2): To 4.48 g (11 mM) of Boc-Acp-Tyr-OMe was added 25 mL of MeOH and 15 mL of 2 M NaOH, and the progress of saponification was monitored by thin layer chromatography (TLC). The reaction mixture was stirred. After 10 h, methanol was removed under vacuum and the residue was taken in 50 mL of water and washed with diethyl ether (2×50 mL). Then the pH of the aqueous layer was adjusted to 2 using 1 m HCl, and it was extracted with ethyl acetate (3×50 mL). The extracts were pooled, dried over anhydrous sodium sulfate, and evaporated under vacuum to yield 3.92 g of **2**. Yield: 3.92 g (10 mM, 90.6%); ^{1}H NMR (300 MHz, [D$_6$]DMSO): δ=12.55 (b, 1H; COOH), 8.01 (d, J=6, 1H; Tyr CONH), 6.99 (d, J=6, 2H; ArH), 6.75–6.73 (t, J=6, 1H; Acp CONH), 6.63 (d, J=9, 2H; ArH), 4.34–4.26 (m, 1H; Tyr C$^{\alpha}$H), 4.06–3.99 (m, 2H; Acp C$^{\varepsilon}$H$_2$), 2.87–2.81 (m, 2H; Tyr C$^{\beta}$H$_2$), 2.74–2.66 (m, 2H; Acp C$^{\alpha}$H$_2$), 2.05–1.99 (m, 2H; Acp C$^{\beta}$H$_2$), 1.36 (s, 9H; (CH$_3$)$_3$C), 1.31–1.28 (m, 2H; Acp C$^{\delta}$H$_2$), 1.19–1.11 ppm (m, 2H; Acp C$^{\gamma}$H$_2$); ESI-MS: 417.57 [M+Na]$^+$, 433.55 [M+K]$^+$; elemental analysis: calcd (%) for $C_{20}H_{30}N_2O_6$ (394): C 60.90, H 7.61, N 7.10; found: C 61.05, H 7.66, N 7.00.

Boc-Acp-Tyr-Glu-OMe (3): A total of 3.54 g (9 mM) of **2** in 10 mL of *N,N*-dimethylformamide was cooled in an ice water bath. H-Glu-OMe was isolated from 4.2 g (20 mM) of the corresponding methyl ester hydrochloride by neutralization, subsequent extraction with ethyl acetate, and concentration (15 mL). This was added to the reaction mixture, followed immediately by 2.08 g (11.11 mM) of DCC and 1.37 g (10.11 mM) of HOBT. The reaction mixture was stirred for 3 days. The residue was taken in ethyl acetate (60 mL), and DCU was filtered off. The organic layer was washed with 2 mL HCl (3×50 mL), brine (3×50 mL), 1 M sodium carbonate (3×50 mL), and brine (2×50 mL), dried over anhydrous sodium sulfate, and evaporated under vacuum to yield the peptide as a white solid. Purification was done by a silica gel column (100–200 mesh) using chloroform/methanol (98:2) as the eluent. Yield: 3.30 g (7 mM, 77.77%); ^{1}H NMR (300 MHz, [D]CHCl$_3$): δ=7.02 (d, J=9, 2H; ArH), 6.96 (d, J=9, 1H; Glu CONH), 6.80 (d, J=9, 2H; ArH), 5.97 (b, 1H; Acp CONH), 4.07–4.67 (m, 1H; Glu C$^{\alpha}$H), 4.60–4.53 (m, 1H; Tyr C$^{\alpha}$H), 3.75 (s, 3H; COOCH$_3$), 3.67 (s, 3H; Glu side chain COOCH$_3$), 3.16–3.05 (m, 2H; Acp C$^{\varepsilon}$H$_2$), 3.03–2.97 (m, 2H; Tyr C$^{\beta}$H$_2$), 2.89–2.81 (m, 2H; Acp C$^{\alpha}$H$_2$), 2.40–2.34 (m, 2H; Glu C$^{\gamma}$H$_2$), 2.23–2.05 (m, 2H; Glu C$^{\beta}$H$_2$), 2.03–1.96 (m, 2H; Acp C$^{\beta}$H$_2$), 1.46 (s, 9H; (CH$_3$)$_3$C), 1.37–1.25 (m, 2H; Acp C$^{\delta}$H$_2$), 1.03–0.96 ppm (m, 2H; Acp C$^{\gamma}$H$_2$); ESIMS: [M+Na]$^+$ 573.99; elemental analysis: calcd (%) for $C_{27}H_{41}N_3O_9$ (551): C, 58.79; H, 7.49; N, 7.62. Found: C, 58.34; H, 7.33; N, 7.28.

Boc-Acp-Tyr-Glu-OH (4): To 2.82 g (6 mM) of Boc-Acp-Tyr-Glu-OMe were added 25 mL of MeOH and 15 mL of 2 M NaOH, and the progress of saponification was monitored by thin-layer chromatography (TLC). The reaction mixture was stirred. After 10 h, methanol was removed under vacuum and the residue was taken in 50 mL of water and washed with diethyl ether (2×50 mL). The pH of the aqueous layer was then adjusted to 2 using 1 M HCl, and it was extracted with ethyl acetate (3×50 mL). The extracts were pooled, dried over anhydrous sodium sulfate, and evaporated under vacuum to yield **4**. Yield: 2.09 g (4 mM, 66.6%); ^{1}H NMR (300 MHz, [D$_6$]DMSO): δ=12.41 (b, 2H; COOH), 8.18 (d, J=6, 1H; Glu CONH), 7.89 (d, J=9, 1H; Tyr CONH), 7.03 (d, J=9, 2H; Ar H), 6.71 (b, 1H; Acp CONH), 6.62 (d, J=6, 2H; Ar H), 4.45–4.43 (m, 1H; Glu C$^{\alpha}$H), 4.22–4.20 (m, 1H; Tyr C$^{\alpha}$H), 4.06–3.99 (m, 2H; Acp C$^{\varepsilon}$H$_2$), 2.90–2.83 (m, 2H; Tyr C$^{\beta}$H$_2$), 2.63–2.55 (m, 2H; Acp C$^{\alpha}$H$_2$), 2.28–2.20 (m, 2H; Acp C$^{\beta}$H$_2$), 2.00–1.98 (m, 2H; Glu C$^{\gamma}$H$_2$), 1.85–1.75 (m, 2H; Glu C$^{\beta}$H$_2$), 1.36 (s, 9H; (CH$_3$)$_3$C), 1.19–1.15 (m, 2H; Acp C$^{\delta}$H$_2$), 1.10–1.08 ppm (m, 2H; Acp C$^{\gamma}$H$_2$); ESIMS: 545.90 [M+Na]$^+$, 561.86 [M+K]$^+$; elemental analysis: calcd (%) for $C_{25}H_{37}N_3O_9$ (523): C 57.35, H 7.12, N 8.30; found: C 57.34, H 7.01, N 8.28.

H$_2$N-Acp-Tyr-Glu-OH (5): To 2.09 g (4 mM) of Boc-Acp-Tyr-Glu-OH was added 5 mL of TFA, and the removal of the Boc group was monitored by TLC. After 2 h, TFA was removed under vacuum. The residue was taken in water (20 mL) and washed with diethyl ether (2×30 mL). The pH of the aqueous solution was then adjusted to 8 with liquid NH$_3$. The aqueous portion was evaporated under vacuum to yield peptide **1** as a white solid. Yield: 1.26 g (3 mM, 75%); $[\alpha]_D^{22}$=6.82 (c=0.58 in water); ^{1}H NMR (300 MHz, [D$_6$]DMSO): δ=8.25 (d, J=6, 1H; Glu CONH), 7.93 (d, J=6, 1H; Tyr CONH), 7.04 (d, J=9, 2H; ArH), 6.63 (d, J=9, 2H; ArH), 4.49–4.44 (m, 1H; Glu C$^{\alpha}$H), 4.25–4.18 (m, 1H; Tyr C$^{\alpha}$H), 2.93–2.88 (m, 2H; Acp C$^{\varepsilon}$H$_2$), 2.82–2.72 (m, 2H; Tyr C$^{\beta}$h$_2$), 2.64–2.55 (m, 2H; Acp C$^{\alpha}$H$_2$), 2.31–2.27 (m, 2H; Acp C$^{\beta}$H$_2$), 2.05–2.01 (m, 2H; Glu C$^{\gamma}$H$_2$), 1.86–1.76 (m, 2H; Glu C$^{\beta}$H$_2$), 1.49–1.33 (m, 2H; Acp C$^{\delta}$H$_2$), 1.08–1.04 ppm (m, 2H; Acp C$^{\gamma}$H$_2$); ^{13}C NMR (75 MHz, [D$_6$]DMSO): δ= 173.78 (COOH), 173.12 (COOH), 171.97 (C=O), 171.87 (C=O), 155.72, 130.96, 128.06, 114.81 (aromatic carbon), 53.95 (Glu C$^{\alpha}$), 51.20 (Tyr C$^{\alpha}$), 36.73 (Acp C$^{\varepsilon}$), 34.93 (Tyr C$^{\beta}$), 30.01 (Acp C$^{\alpha}$), 26.76 (Acp C$^{\delta}$), 26.35 (Glu C$^{\gamma}$), 25.28 (Glu C$^{\beta}$), 24.63 ppm (Acp C$^{\gamma}$); ESIMS: 446.08 [M+Na]$^+$, 468.04 [M+K]$^+$, 424.04 [M+H]$^+$; elemental analysis: calcd (%) for $C_{20}H_{29}N_3O_7$ (423): C 56.73, H 6.90, N 9.92; found: C 56.34, H 6.33, N 9.28.

Experiments

NMR experiments: NMR studies were carried out on a Brüker DPX 300 MHz spectrometer at 300 K. Compounds concentrations were in the range 1–10 mmol in CDCl$_3$ and [D$_6$]DMSO

Mass Spectroscopy: Mass spectra were recorded on a HEWLETT PACKARD series 1100MSD and Micromass Qtof micro YA263 mass spectrometer by positive mode electron spray ionisation.

Dynamic light Scattering (DLS) experiment: DLS has been done in Nano ZS MALVERN Instrument UK using solution of different peptide concentration.

Circular Dichroic (CD) study: CD study has been carried out on a JASCO J-815-150S instrument at a temperature of 25 °C.

Polarimeter: Perkin–Elmer instruments. Model 341 LC polarimeter.

Fourier Transform IR (FT-IR) spectroscopy: The FT-IR spectra were taken using Shimadzu (Japan) model FT-IR spectrophotometer. Peptide solutions were suspended on a CaF$_2$ plate and dried by vacuum. The peptide deposits were resuspended with D$_2$O and subsequently dried to form thin films and spectra were collected at 25 °C.

Transmission electron microscopy (TEM) and field-emission scanning electron microscopy (FE-SEM): TEM and FE-SEM were carried out to investigate the morphology of the nanostructures. In general, solutions of peptide at different concentration were taken and a drop of the solution was placed on a carbon-coated copper grid (300 mesh) and evaporated. Again, a drop of uranil acetate solution (freshly prepared 2% uranil acetate solution) was added and dried under vacuum for 10 h. With these grids, TEM studies were carried out using a JEOL JEM 2010 electron microscope. During SEM, a solution of the reported peptide was taken on glass cover slips and evaporated to dryness for 24 h. A gold coating was applied on the top of the sample to make it conductive for analysis. It was studied on a JEOL JSM 6007F instrument at 3.0 KV voltage and 20000× magnification.

Atomic force microscopic (AFM) study: The peptide solution was dried by slow evaporation on a microscopic cover glass and then atomic force

microscopic (AFM) study was performed using an AUTOPROBE CP BASE UNIT, di CP-II instrument, Model no. AP-0100 instrument.

Fluorescence microscopic study: Fluorescence microscopic study was carried out using a LEICA DM 1000 fluorescence microscope at 60× magnification.

Acknowledgements

J.N. wishes to acknowledge the CSIR, New Delhi, India, for financial assistance. We also thankfully acknowledge Nanoscience and Technology Initiatives, DST, Government of India, New Delhi.

[1] a) G. M. Whitesides, J. P. Mathias, C. T. Seto, *Science* **1991**, *254*, 1312–1319; b) *Supramolecular Chemistry: Concepts and Perspectives* (Ed.: J. M. Lehn), Wiley-VCH, Weinheim, Germany, **1995**.

[2] a) S. Bhattacharya, S. De, *Chem. Eur. J.* **1999**, *5*, 2335–2347; b) C. H. Görbitz, *New J. Chem.* **2003**, *27*, 1789–1793; c) T. Rehm, V. Stepanenko, X. Zhang, F. Würthner, F. Gröhn, K. Klein, C. Schmuck, *Org. Lett.* **2008**, *10*, 1469–1472; d) M. Gupta, A. Bagaria, A. Mishra, P. Mathur, A. Basu, S. Ramakumar, V. S. Chauhan, *Adv. Mater.* **2007**, *19*, 858–861; e) S. Ghosh, M. Raches, E. Gazit, S. Verma, *Angew. Chem.* **2007**, *119*, 2048–2050; *Angew. Chem. Int. Ed.* **2007**, *46*, 2002–2004; f) A. Mishra, J. J. Panda, A. Basu, V. S. Chauhan, *Langmuir* **2008**, *24*, 4571–4576; g) C. H. Görbitz, *Chem. Eur. J.* **2001**, *7*, 5153–5159; h) S. Ray, D. Halder, M. G. B. Drew, A. Banerjee, *Org. Lett.* **2004**, *6*, 4463–4465.

[3] a) Y. Song, S. R. Challa, C. J. Medforth, Y. Qiu, R. K. Watt, D. Pena, J. E. Miller, F. Swol, J. A. Shelnutt, *Chem. Commun.* **2004**, 1044–1045; b) S. Vauthey, S. Santoso, H. Gong, N. Watson, S. Zhang, *Proc. Natl. Acad. Sci. USA* **2002**, *99*, 5355–5360; c) M. Reches, E. Gazit, *Science* **2003**, *300*, 625–627; d) X. Gao, H. Matsui, *Adv. Mater.* **2005**, *17*, 2037–2050; e) J. D. Hartgerink, E. Beniash, S. I. Stupp, *Science* **2001**, *294*, 1684–1688; f) S. Santoso, W. Hwang, H. Hartman, S. Zhang, *Nano Lett.* **2002**, *2*, 687–691.

[4] a) D. T. Bong, T. D. Clark, J. R. Granja, M. R. Ghadiri, *Angew. Chem.* **2001**, *113*, 1016–1041; *Angew. Chem. Int. Ed.* **2001**, *40*, 988–1011; b) C. H. Görbitz, M. Nilsen, K. Szeto, L. W. Tangen, *Chem. Commun.* **2005**, 4288–4290.

[5] a) N. Kol, L. Abramovich, D. Barlam, R. Z. Shneck, E. Gazit, I. Rousso, *Nano Lett.* **2005**, *5*, 1343–1346.

[6] M. Yemini, M. Reches, J. Rishpon, E. Gazit, *Nano Lett.* **2005**, *5*, 183–186.

[7] B-S. Kim, D.-J. Hong, J. Bae, M. Lee, *J. Am. Chem. Soc.* **2005**, *127*, 16333–16337.

[8] A. Ajayaghosh, R. Varghese, S. Mahesh, V. K. Praveen, *Angew. Chem.* **2006**, *118*, 7893–7896; *Angew. Chem. Int. Ed.* **2006**, *45*, 7729–7732.

[9] M. Reches, E. Gazit, *Nano Lett.* **2004**, *4*, 581–585.

[10] P. P. Bose, A. K. Das, R. P. Hegde, N. Shamala, A. Banerjee, *Chem. Mater.* **2007**, *19*, 6150–6157.

[11] X. Yan, Q. He, K. Wang, L. Duan, Y. Cui, J. Li, *Angew. Chem.* **2007**, *119*, 2483–2486; *Angew. Chem. Int. Ed.* **2007**, *46*, 2431–2434.

[12] X. Yan, Y. Cui, Q. He, K. Wang, J. Li, W. Mu, B. Wang, Z. Ou-yang, *Chem. Eur. J.* **2008**, *14*, 5974–5980.

[13] C. Wang, S. Yin, S. Chen, H. Xu, Z. Wang, X. Zhang, *Angew. Chem.* **2008**, *120*, 9189–9192; *Angew. Chem. Int. Ed.* **2008**, *47*, 9049–9052.

[14] a) S. Guha, M. G. B. Drew, A. Banerjee, *Chem. Mater.* **2008**, *20*, 2282–2290; b) D. Haldar, A. Banerjee, M. G. B. Drew, A. K. Das, A. Banerjee, *Chem. Commun.* **2003**, 1406–1407.

[15] S. Ghosh, S. K. Singh, S. Verma, *Chem. Commun.* **2007**, 2296–2298.

[16] C. L. Stevenson, M. M. Tan, D. L. Ballesteros, *J. Pharm. Sci.* **2003**, *92*, 1832–1843.

[17] M. Crisma, G. D. Fasman, H. Balaram, P. Balaram, *Int. J. Pept. Protein Res.* **1984**, *23*, 411–419.

[18] M. Raches, E. Gazit, *Phys. Biol.* **2006**, *3*, S10–S19.

[19] a) M. Antonietti, S. Förster, *Adv. Mater.* **2003**, *15*, 1323–1333; b) I. P. Kaur, A. Garg, A. K. Singla, D. Aggarwal, *Int. J. Pharm.* **2004**, *269*, 1–14; c) T. Merdan, J. Kopecek, T. Kissel, *Adv. Drug Delivery Rev.* **2002**, *54*, 715–758.

Received: July 14, 2009
Published online: November 17, 2009

